Search for cosmic strings in the COSMOS survey

J. L. Christiansen, E. Albin, T. Fletcher, J. Goldman, I. P. W. Teng, M. Foley, and G. F. Smoot

Search for Cosmic Strings in the COSMOS Survey

J. L. Christiansen,* E. Albin, and T. Fletcher

Department of Physics, California Polytechnic State University, San Luis Obispo, California 93407, USA

J. Goldman and I.P.W. Teng

Department of Physics, National University of Singapore, Singapore 117542

M. Foley

Department of Biomedical Engineering, California Polytechnic State University, San Luis Obispo, California 93407, USA

G. F. Smoot

Lawrence Berkeley National Laboratory, Space Sciences Laboratory
and Department of Physics, University of California, Berkeley, California 94720, USA
(Dated: April 8, 2011)

We search the COSMOS survey for pairs of galaxies consistent with the gravitational lensing signature of a cosmic string. The COSMOS survey imaged 1.64 square degrees using the Advanced Camera for Surveys (ACS) aboard the Hubble Space Telescope (HST). Our technique includes estimates of the efficiency for finding the lensed galaxy pair. We find no evidence for cosmic strings with a mass per unit length of $G\mu/c^2 < 3.0 \times 10^{-7}$ out to redshifts greater than 0.6 and set 95% upper limits. This corresponds to a global 95% upper limit of $\Omega_{strings} < 0.0028$.

PACS numbers: 98.80.Cq

I. INTRODUCTION:

Cosmic strings are linear topological defects that arise naturally during symmetry-breaking phase transitions in the early universe [1, 2]. They have also been proposed in string theory models of inflation, occuring just after the GUT scale transition [3]. Detailed simulations of the dynamics and interactions of cosmic strings predict a modern day stochastic network of strings, observable through a variety of astrophysical phenomena [4, 5]. The dimensionless scale of observational interest is $G\mu/c^2 \lesssim 10^{-6}$ where μ is the string energy-density [6].

Despite considerable interest within the theory community and multiple proposed production mechanisms, only a few observations bear on the subject, including cosmic microwave background (CMB) [7–11], gravitational waves [12–14], and gravitational lensing [15, 16]. The CMB power spectrum shows that cosmic strings are not the dominant factor in large-scale structure formation, but that they may contribute up to about 10% of the observed structure, enough to possibly detect with the Planck data [17, 18] or other experiments with resolution on small angular scales [19].

Gravitational lensing of background galaxies by a cosmic string is expected to produce a pair of images separated by an angle, $\Delta\theta = \delta \sin(\beta)D_{ls}/D_{os}$ where $\delta = 8\pi G\mu/c^2$ is the deficit angle, D_{ls} is the distance between the lensing string (l) and the background source (s), D_{os} is the distance between the observer (o) and the background source, and β is the tilt of the string toward the observer.

In our previous search for gravitational lensing by cosmic strings in the GOODS survey we concluded with 95% confidence that $G\mu/c^2 < 3.0 \times 10^{-7}$ out to redshifts greater than 0.5 and that $\Omega_{strings} < 0.02$ [15]. Our aim in this paper is to use the same technique to analyze the wider survey carried out by the COSMOS team with the Hubble Space Telescope (HST) Advanced Camera for Surveys (ACS). This survey has a field-of-view that is 24 times larger than the GOODS survey and the limits we find are nearly 10 times lower than our previous limits. Because strings are linear objects and backgrounds scale with the field-of-view, we have found it necessary to perform the search in four angular bins to improve the signal-to-noise ratio.

In Section II we describe our data selection and present the correlation analysis used to search for cosmic strings in the COSMOS survey. We discuss the simulations needed to estimate the signal rates and detection efficiencies in Section III. These estimates are then used in Section IV to determine limits on individual cosmic strings as a function of mass and redshift as well as the global limit on the density of cosmic strings. Finally, we summarize our results in Sec. V.

II. DATA SAMPLE:

The COSMOS field is 1.64 degrees^2 centered on RA=10:00:28.6 and DEC=+02:12:21.0. Images were taken with the ACS aboard HST between July 2003 and June 2005 [20, 21]. We analyze the publicly available COSMOS Version 1.3 data in the F814W (I-band) filter which consists of 81 drizzled tiles with a resolution of

*Electronic address: jlchrist@calpoly.edu

0.05 ″/pixel. We apply a fiducial cut and use the central 1.57 degrees^2 of the survey.

A. Source identification

We use SExtractor version 2.5.0 (Source Extractor) to identify sources in the COSMOS survey [22, 23] following the *Hot* procedure outlined in [24]. For shape-sensitive analyses like weak lensing, Leauthaud et al. advocate a *Hot-Cold* method applied to un-rotated, undrizzled images. We validate our *Hot* catalogs against the public release of the well-understood Leauthaud et al. catalog containing 1.2 million objects which we refer to as the *LC2* catalog described in [24]. We do not perform a catalog-level search using the *LC2* catalog directly due to the difficulties in estimating the efficiency of finding lensed galaxies without access to the original COSMOS fits images and processing pipeline.

Several minor modifications need to be applied to Leauthaud's *Hot* parameters [24] to account for the difference in resolution for the publicly available tiles. We set the PIXEL_SCALE to 0.5 arcsec, use a gaussian filter width of 2.5 pixels, and set the DETECT_MINAREA to 9 contiguous pixels above threshold. We also scale the apertures to 12 pixels, PHOT_APERTURES and PHOT_AUTOAPERS. Finally, to reduce the deblending slightly, we set the DEBLEND_NTHRESH to 32 and the DEBLEND_MINCONT to 0.1. The resulting catalog contains 812,463 objects with magnitudes brighter than 26.5.

B. Resolved galaxy selection

We select the resolved galaxies from this sample using the correlation of the peak surface brightness, MU_MAX, with the objects magnitude, MAG_AUTO. Fig. 1 shows three regions of interest in the MU_MAX vs MAG_AUTO plane: resolved galaxies, point sources including stars, and spurious detections where the objects are too small to be consistent with the point spread function. There are 761,370 resolved galaxies, 36,823 point sources, and 14,270 spurious detections. The *LC2* catalog contains fewer spurious detections due to a prior cleaning procedure that included merging of small objects with nearby objects from the *Cold* catalog and removal of objects in regions of elevated noise that occur on the borders of the un-rotated tiles as well as near bright stars. To reproduce the additional "by hand" cleaning, we correlate our resolved galaxies with the *LC2* catalog.

We find that 96.4% of the resolved galaxies with magnitudes brighter than 23rd magnitude are also found in the *LC2* catalog. Our magnitudes generally agree, but have a tail down to smaller values which we attribute to over deblending of larger objects. The 3.6% of events that don't have a counterpart in the *LC2* catalog are all found in the diffraction trails of very bright stars or in a few cases near the edge of the survey consistent with
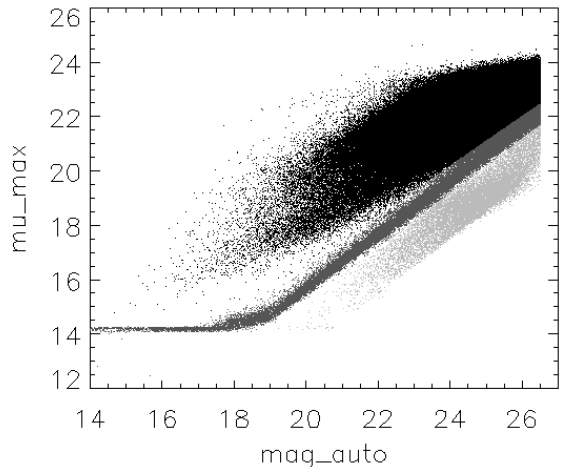

FIG. 1: Resolved galaxies (black points) are a distinct population. Also shown are point sources (dark gray) including stars, and spurious objects (light gray) that are too small to be consistent with the PSF.

the more aggressive cleaning. The situation is understandably slightly worse for dimmer objects; 87.7% of the galaxies at 25th magnitude have a counterpart in the *LC2* catalog. The magnitudes tend to agree well. The 12.3% of galaxies that don't have a counterpart in the *LC2* catalog are again in fiducial regions that were removed by hand. For the rest of the galaxies, most of them are in regions with elevated noise. Very few appear to be legitimate detections.

To reproduce the cleaning as much as possible, we remove resolved sources in our catalog that are not included in the *LC2* catalog. This removes about 11.6% of our resolved galaxies. Any inefficiency that comes about from this requirement is included in our efficiency estimate. More importantly, though, this requirement protects us from overestimating the cosmic string lensing rate due to spurious detections.

We post-process our resolved galaxy catalog to identify the pixels in the image associated with each galaxy. First we define a small but encompassing search region about each galaxy centroid. This region is chosen to be three times the size of the galaxy reported by the catalog coordinates (XMIN_IMAGE, YMIN_IMAGE) and (XMAX_IMAGE, YMAX_IMAGE). Next we determine the local background characteristics by fitting a gaussian to the small amplitude peak in a histogram of the pixel intensities. Finally, we find a bright pixel near the galaxy centroid and iteratively aggregate neighboring pixels that are 1σ above the mean background. This process occasionally merges neighboring galaxies. In the event that a cluster of pixels reaches the edge of the search region or that two galaxies merge, we raise the neighbor threshold to 2σ above the mean background and repeat the process. We continue to raise the threshold until each galaxy is completely con-

tained within the search region and does not contain the centroid from any other galaxy in the catalog. The aim of this procedure is to retain as much unbiased shape information as possible. For 0.15% of the dimmest sources the threshold is raised so high that there are no pixels left in the cluster and we remove these galaxies from the sample. After selecting resolved galaxies also identified in the *LC2* catalog and identifying the galaxy pixels, the resulting catalogs contain 662,765 resolved galaxies.

C. Matched galaxy pair selection

The morphological similarity between each pair of galaxies is characterized by the correlation and cross-correlation of the two galaxy images [15]. We first align the centroids and then calculate the correlation ($CORR$) and the cross-correlation ($XCORR$) of the pixel intensities.

$$CORR = \frac{\sum I_1(x_i, y_i)^2 - \sum I_2(x_i, y_i)^2}{\sum I_1(x_i, y_i)^2 + \sum I_2(x_i, y_i)^2} \qquad (1)$$

$$XCORR = \frac{2 \sum I_1(x_i, y_i) * I_2(x_i, y_i)}{\sum I_1(x_i, y_i)^2 + \sum I_2(x_i, y_i)^2} \qquad (2)$$

where $I(x_i, y_i)$ is the intensity of each pixel in a galaxy and the subscript 1 or 2 refers to the galaxies being correlated. Galaxies with $CORR$ near a value of zero have very similar magnitudes and galaxies with $XCORR$ near a value of one are similar in surface brightness and shape. We define matched galaxy pairs as those within the ellipse defined by

$$\sqrt{(2 * CORR)^2 + (1 - XCORR)^2} < 0.29 \qquad (3)$$

This cut was optimized on simulated lensing events and is slightly looser than the one used in our previous GOODS search.

In this analysis, we consider pairs of galaxies with opening angles, $\Delta\theta < 15''$. There are 96,413 matched pairs out of 7,081,011 total pairings with $\Delta\theta < 15''$ in the COSMOS survey. The selected matched pairs are consistent with the null hypothesis.

D. Pairs distribution

The binned distribution of matched galaxy pairs is shown in Fig. 2. The distribution is divided into four overlapping angular bins: -5°:50°, 40°:95°, 85°:140°, and 130°:185°. The angular bins correspond to a range of cosmic string angles on the sky. The hypothetical string is presumed to pass between the two galaxies in a pair at an angle perpendicular to the line connecting the galaxy centroids. These bins are needed to reduce the background as the survey gets increasingly large. Because cosmic strings are linear objects, the signal scales with
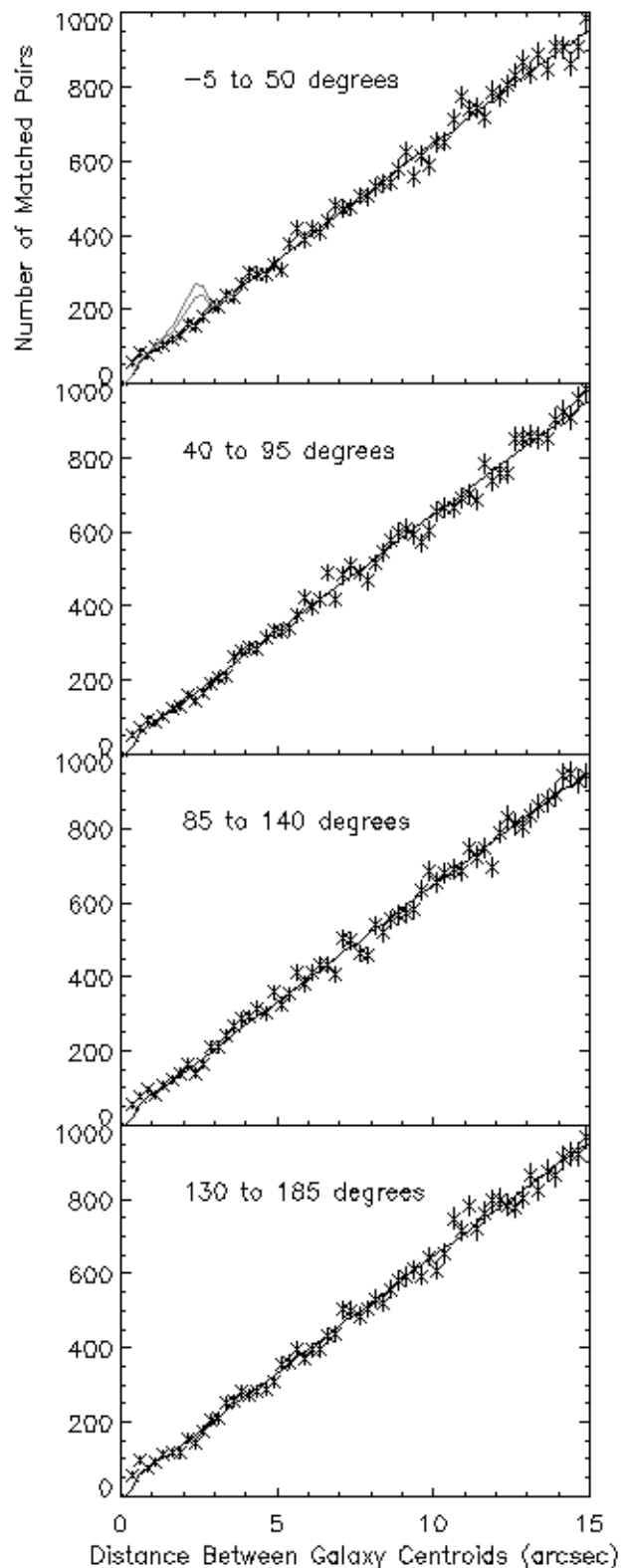

FIG. 2: Pairs of galaxies in four angular bins (points) are compared to background (solid line). The top panel shows one example of a simulated string (grey). The upper simulated string is the total number of pairs expected from the simulation with string length of 1.19^o, redshift of 0.5, and $\delta \sin\beta$ of 4$''$. The lower simulated string includes measurement inefficiencies.

the width of the survey whereas the background scales with the area of the survey. We do not want to restrict our search to perfectly straight strings so we keep the number of bins to a minimum. Overlapping bins are chosen to assure us that we are searching efficiently.

The background shape is characterized by the distribution of all pairs of galaxies regardless of size and shape. Because strings with masses large enough to create opening angles greater than $7''$ have been ruled out, we normalize the background distribution to the number of measured matched pairs between $7''$ and $15''$. This gives us a reliable estimate of the background at smaller opening angles. From the background, we observe that SExtractor merges galaxies with opening angles below $0.4''$.

In our signal region, between $0.4''$ and $7''$, there are 24 data bins and the $\chi^2/24 - dof$ of the matched pairs to the background is 0.99, 1.1, 1.3, and 1.4 for the four angular bins respectively. The p-values range from 15% to 48%. Based on the scaled background distribution, we report no evidence for an excess of pairs at small opening angles. Although there is no statistically significant excess in our signal region, we note that there is a small excess of signal below $1''$ and that the first data point in the signal region is systematically high. This excess is consistent with the fact that the dimmest galaxies tend to pass the correlation cuts more easily than larger galaxies. To investigate this region more carefully, we surveyed matched pairs with opening angles less than $1''$ by hand. We find that matched pairs tend to be discovered in regions of high galaxy density and that these regions tend to have other lensing candidates at the fairly high rate of $0.5/1'$. A full statistical analysis of these pairs shows no evidence of lensing and gives us a calibration curve for the background in high density regions.

III. COSMIC STRING SIMULATIONS:

Simulations are used to estimate both the number of lensed galaxy pairs based on the local density of galaxies in the COSMOS survey as well as the efficiency of finding those pairs. The simulation of lensed galaxy pairs is the same as used previously in our GOODS search [15]. The idea is to use the density of galaxies in our catalog of sources to monte carlo the number of pairs that would exist from any theoretical string crossing our survey. An important aspect of this calculation is the simulation of the galaxy redshifts. We use the same parameterization of the redshift distribution as [25]. For these studies, COSMOS tile 55 is used as a typical example. The simulated redshift distribution of the galaxies in this tile is shown in Fig. 3.

The advantage of a catalog-level signal simulation is that we can quickly embed as many strings as needed to get an accurate estimate of the average number of lensed galaxies observed from a particular set of string parameters, including redshift and $\delta \sin \beta$. An example
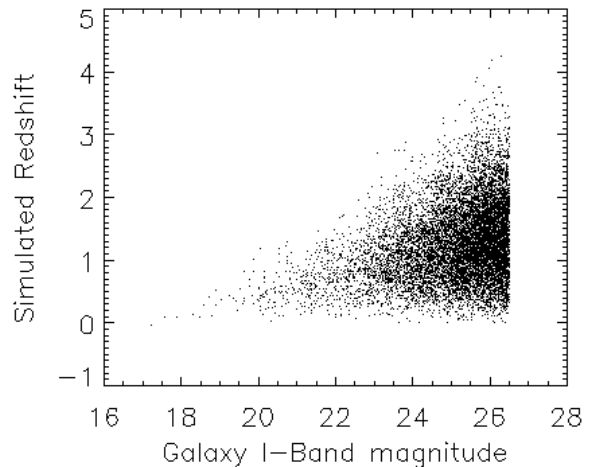

FIG. 3: The simulated redshift distribution for galaxies in a typical COSMOS tile.

of the result from this simulation is shown in the top panel of Fig. 2.

Fig. 4 summarizes the efficiencies as a function of the opening angle between the galaxies and the string redshift. These efficiencies were estimated by embedding galaxies as realistically as possible into COSMOS tiles and then processing the modified tiles back through our analysis chain to see how many embedded sources are found. The curves include both the efficiency of identifying the embedded galaxies with SExtractor and the correlation and cross correlation selection cuts. Below $0.4''$ galaxies are merged by SExtractor and the pair is lost. For dim galaxies, which tend to have higher redshifts, noise in the galaxy detection becomes an increas-
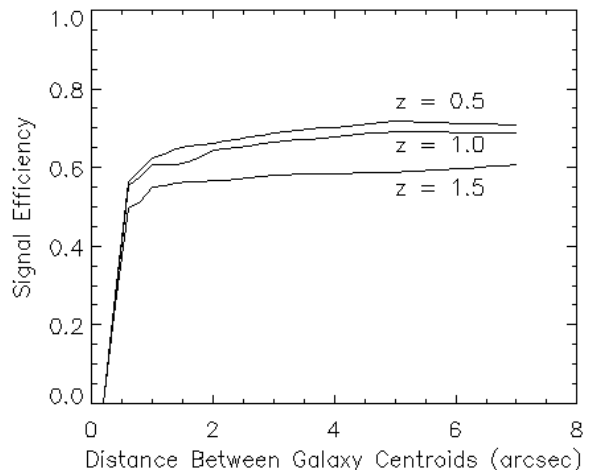

FIG. 4: Efficiency of detecting pairs of galaxies lensed by a cosmic string as a function of pair opening angle and redshift.
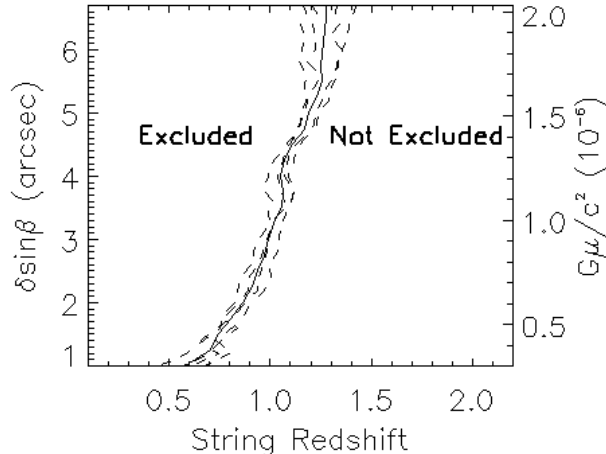
FIG. 5: 95% upper limits for lensed galaxies produced by a cosmic string as a function of the string mass and redshift. Dashed lines are the individual limits from each angular bin shown above. The solid line is the average limit for all directions.

ingly important effect.

IV. RESULTS:

The distribution of matched galaxy pairs shown in Fig. 2 rises nearly linearly. This is expected for the background pairs and any excess above the background could be evidence of a cosmic string. For comparison, simulated pairs from a cosmic string at a redshift of 0.5 and $\delta \sin \beta$ of $4''$ are included in the top panel. They are normalized to the mean length of a string crossing the survey, 1.19^o. The upper curve is the total simulated signal. The lower curve includes the detection inefficiencies from Fig. 4.

We compare a wide variety of predicted cosmic string signals to the data to determine limits. Signal pairs, n_s, are summed from $0.4''$ to a maximum opening angle beyond which there is no more signal. The observed matched pairs, n_{obs}, and the background, n_{bkg}, from Fig. 2 are summed over the same range of opening angles. We then compute the single-sided Neyman 95% confidence limit, n_{lim}, which is the minimum signal that is consistent with background fluctuations. Signals with $n_s > n_{lim}$ are excluded by the data. The resulting 95% upper limits are shown in Fig. 5. All four angular bins yield similar limits that extend from $1'' < \delta \sin \beta < 7''$. We average the four angular bins for the global limit. Taking the mean tilt of a string with respect to the observer to be $< \sin \beta > = 2/\pi$ we relate the opening angle to the mass scale via the factor $8\pi \frac{G\mu}{c^2} = \delta < \sin \beta >$ shown on the right-hand axis. We see no evidence for cosmic strings out to a redshift greater than 0.5 and place a 95% upper limit of $G\mu/c^2 < 3.0 \times 10^{-7}$.
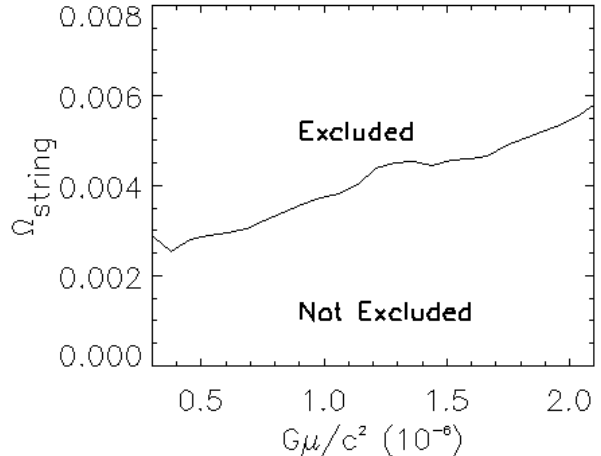

FIG. 6: 95% upper limits on the global parameter, $\Omega_{strings}$, as a function of the string mass.

If strings are rare occurrences, it is likely that none would appear in the COSMOS field (fov = 1.57 degrees^2) and that other surveys may yield different results. Because strings are line-like objects, we expect that the COSMOS field of view would intersect a single string about 0.5% of the time. Using a simple geometric monte-carlo we determine that approximately 820 straight strings randomly placed in a volume of comoving radius, η, are needed for a 95% detection rate in a COSMOS fov. In this case, the average COSMOS fov contains 3 detectable string crossings as expected from Poisson statistics. This string density corresponds to a total length of string, $L_{tot} = 1200\eta$, in the volume and we use the invariance of L_{tot}/η to set limits on $\Omega_{strings}$.

$$\Omega_{strings} = \frac{\mu(L_{tot}/\eta)\eta}{(4/3)\pi\eta^3} \times \frac{8\pi G}{3H_0^2} \qquad (4)$$

where η is the comoving distance computed with $h = 0.7$, $\Omega_M = 0.27$, and $\Omega_\Lambda = 0.73$. Fig. 6 shows the string densities excluded by this method. The limit excludes a string density that is 0.28% of the critical density for the smallest mass strings and rises to 0.4% for more massive strings. Each limit assumes that all cosmic strings have the same $G\mu/c^2$ as predicted by some models. Because non-uniform string networks are predicted to have a very steep spectral index, (-10<index<-6) [5], strings at the measurement threshold will dominate the sensitivity.

A wide variety of theoretical models predict $\Gamma = \Omega_{strings}/(8\pi G\mu)$ of order 10 [5]. Our measurement is consistent with $\Gamma = 375$ for low-mass strings and $\Gamma = 110$ for our largest-mass strings and thus indicates that we are not yet sensitive to masses of current theoretical interest.

V.   CONCLUSION:

We have used the COSMOS survey field to search for cosmic strings. We find no evidence for the gravitational lensing signature. We have included the observational efficiencies in our analysis using the same technique we used previously on the GOODS survey. Figs. 5 and 6 summarize our results. We set 95% upper limits of $G\mu/c^2 < 3.0 \times 10^{-7}$ out to redshifts greater than 0.6 which leads in turn to a global limit of $\Omega_{strings} < 0.0028$. We note that, while these results have as their foundation the hypothesis of long straight strings, they also exclude strings with moderate curvature.

The global limit on $\Omega_{strings}$ is nearly 10 times stronger than our previously published limit [15]. We want to emphasize that our technique is complementary to other methods. We excluded masses that are smaller than those excluded by other direct CMB searches [11]. However, our masses are larger than those reported by parameter fits to the CMB [7–10] as well as gravitational wave searches [12, 13]. The recent microlensing search carried out on SDSS quasars [16] is sensitive to very low-mass strings, but reports a similar sensitivity for $\Omega_{strings}$. Our direct searches may be sensitive to a particular class of strings that could be missed by other searches.

VI.   ACKNOWLEDGEMENTS:

[1] T. Kibble, J. Phys. A **9**, 1387 (1976).
[2] J. Polchinski, hep-th/0412244.
[3] M. Sakellariadou, hep-th/0602276.
[4] M. Hindmarsh and T. Kibble, Rep. Prog. Phys. **58**, 477 (1995).
[5] S.-H. H. Tye, I. Wasserman, and M. Wyman, Phys. Rev. **D71**, 103508 (2005).
[6] E. Copeland and T. Kibble, Proc. Roy. Soc. Lond. **A**, 623 (2010).
[7] M. Wyman, L. Pogosian, and I. Wasserman, Phys. Rev. **D73**, 089905 (2006).
[8] M. Wyman, L. Pogosian, and I. Wasserman, Phys. Rev. **D72**, 023513 (2005).
[9] N. Bevis, M. Hindmarsh, M. Kunz, and J. Urrestilla, Phys. Rev. Lett **100**, 021301 (2008).
[10] R. Battye and A. Moss, Phys. Rev. **D82**, 023521 (2010).
[11] E. Jeong and G. Smoot, Astrophys. J. **624**, 21 (2005).
[12] F. Jenet et al., Astrophys. J. **653**, 1571 (2006).
[13] B. Abbott et al., Phys. Rev. **D80**, 062002 (2009).
[14] B. Abbott et al., Nature **460**, 990 (2009).
[15] J. L. Christiansen et al., Phys. Rev. **D77**, 123509 (2008).
[16] A. Tuntsov and M. Pshirkov, Phys. Rev. **D81**, 063523 (2010).
[17] E. Jeong, C. Baccigalupi, and G. Smoot, arXiv:1004.1046.
[18] N. Bevis, M. Hindmarsh, M. Kunz, and J. Urrestilla, arXiv:1005.2663v1.
[19] L. Pogosian, S.-H. Tye, I. Wasserman, and M. Wyman, J. Cosmol. Astropart. **0902**, 013 (2009).
[20] N. Scoville et al. (2007).
[21] A. Koekemoer et al., ApJS **172**, 196 (2007).
[22] E. Bertin, *Sextractor v2.4 user's manual* (2005).
[23] E. Bertin and Arnouts, Astron. and Astron. Suppl. Ser. **117**, 393 (1996).
[24] A. Leauthaud et al., ApJS **172**, 219 (2007).
[25] R. Massey et al., Astron.J. **127**, 3089 (2004).